Subgrid-scale modeling of turbulence-chemistry interaction for hypersonic boundary layers in chemical nonequilibrium

By C. T. Williams

1. Motivation and objectives

Hypersonic flight vehicles are subject to significant aerodynamic heating due to the presence of several hydrodynamic phenomena, including the formation of leading-edge shock waves, viscous dissipation in compressible boundary layers, shock-interference heating, and shock-boundary layer interactions (Urzay 2018; Candler 2019; Urzay & Di Renzo 2020). The high temperatures introduced by these phenomena activate several nonequilibrium thermochemical processes, including vibrational-electronic energy excitation, chemical dissociation of diatomic species, and, for sufficiently high enthalpies, ionization reactions within the shock layer (Vincenti & Kruger 1965; Park 1990; Bertin & Cummings 2006). As these thermochemical processes are strongly endothermic, predicting the rate at which they proceed is fundamental for determining the thermal field surrounding and hence heat flux into hypersonic vehicles. Owing to the similarity in characteristic timescales for turbulent motion and the aforementioned endothermic processes in hypersonic boundary layers, turbulence-induced thermodynamic fluctuations will modify the chemical production rates and thus chemical heat release. Therefore, in the context of coarse-grained simulations of turbulent hypersonic boundary layers, modeling of the subfilter chemical production rates is crucial not only for the prediction of the boundary-layer chemical composition but also for the spatial variation of the temperature field and corresponding heat fluxes.

Characterization of turbulence-chemistry interaction in temporally evolving hypersonic boundary layers was first performed by Duan & Martín (2011a,b), who confirmed the strong sensitivity of the chemical production rates to turbulent fluctuations. Corresponding efforts to model this turbulence-chemistry interaction in the context of coarse-grained simulations have focused largely on capturing the impact of thermal fluctuations alone (Martín & Candler 1999; Duan & Martín 2011a), neglecting correlated fluctuations in the remaining thermodynamic state variables. The generality of this modeling assumption, however, remains unsubstantiated in reacting hypersonic boundary layers. The dual objectives of the present study are then as follows: first, to disambiguate the relative impact of fluctuations in each of the thermochemical state variables on the mean chemical production rates in turbulent hypersonic boundary layers, and second, to present and evaluate *a-priori* a fully dynamic subgrid-scale model for turbulence-aerothermochemistry interactions.

The remainder of this brief is structured as follows. Section 2 analyzes in detail turbulence-chemistry interactions in a strongly reacting hypersonic boundary layer, establishing the relative impact of turbulent fluctuations in each of the thermodynamic variables. A dynamic subgrid-scale model for hypersonic turbulence-chemistry interac-

tions is developed and assessed *a priori* in Section 3. Finally, Section 4 draws conclusions and proposes directions for further research.

2. Analysis of turbulence-chemistry interaction

In order to investigate in detail turbulence-aerothermochemistry interactions in hypersonic boundary layers, the analysis in this subsection focuses on the direct numerical simulation (DNS) results of Williams *et al.* (2023). The direct simulation was performed with the HTR solver (Di Renzo *et al.* 2020; Di Renzo & Urzay 2021), accounting for multi-component diffusion and finite-rate chemistry (Park 1990), utilizing a high-order, low-dissipation hybrid TENO6/skew-symmetric scheme (Williams *et al.* 2022) for the evaluation of inviscid fluxes. For compactness and consistency, this brief adopts the same mathematical notation and variable definitions introduced by Williams *et al.* (2023).

As a result of the comparable timescales between the chemical production rates and turbulent motion observed in the hypersonic boundary layer, turbulent fluctuations in the thermodynamic state variables significantly impact the reaction rates. In the context of Reynolds-averaged Navier Stokes simulations, this turbulence-chemistry interaction manifests itself in departures of the averaged chemical production rates from the chemical production rates evaluated at the mean thermochemical state, i.e., $\langle \dot{w}_i \rangle \neq \dot{w}_i(\langle\rho\rangle, \langle T\rangle_f, \langle Y_j\rangle_f)$ in general due to the strong nonlinearity of the reaction rates. The objective of this subsection is, first, to assess *a priori* the magnitude of the turbulence-chemistry interactions, and second, to identify the relative impact of individual thermodynamic fluctuations on the mean chemical production rate for each of the species present in partially dissociated air. To that end, the so-called laminar closure for the reactive source terms is introduced as

$$\mathcal{W}_i^{(I)} := \dot{w}_i(\langle\rho\rangle, \langle T\rangle_f, \{\langle Y_j\rangle_f\}) = \int_\Omega d\Omega\ \dot{w}_i(\rho, T, \{Y_j\})\mathcal{P}_l, \tag{2.1}$$

where Ω is the sample space of thermodynamic state variables from the DNS, and $\mathcal{P}_l = \delta(\rho - \langle\rho\rangle)\delta(T - \langle T\rangle_f)\prod_{j=1}^{N_s}\delta(Y_j - \langle Y_j\rangle_f)$ is the implied probability density function (PDF) for the laminar closure. In order to assess the importance of specific thermodynamic fluctuations on the chemical production rates, let us introduce auxiliary chemical-production variables

$$\mathcal{W}_i^{(II)} := \int_\Omega d\Omega\ \dot{w}_i(\langle\rho\rangle, T, \{Y_j\})\mathcal{P}(T, \{Y_j\}), \tag{2.2}$$

$$\mathcal{W}_i^{(III)} := \int_\Omega d\Omega\ \dot{w}_i(\rho, \langle T\rangle_f, \{Y_j\})\mathcal{P}(\rho, \{Y_j\}), \tag{2.3}$$

$$\mathcal{W}_i^{(IV)} := \int_\Omega d\Omega\ \dot{w}_i(\rho, T, \{\langle Y_j\rangle_f\})\mathcal{P}(\rho, T), \tag{2.4}$$

corresponding to the mean chemical production rates absent density, temperature, and mass-fraction fluctuations, respectively. In this formulation, $\mathcal{P}$ denotes the (joint) PDF corresponding to the set of thermodynamic state variables taken as arguments. In order to characterize the extent to which the statistical dependence of fluctuations in thermodynamic states variables impacts the mean production rate, a final auxiliary variable is introduced as

$$\mathcal{W}_i^{(V)} := \int_\Omega d\Omega\ \dot{w}_i(\rho, T, \{Y_j\})\mathcal{P}(\rho)\mathcal{P}(T)\mathcal{P}(\{Y_j\}), \tag{2.5}$$

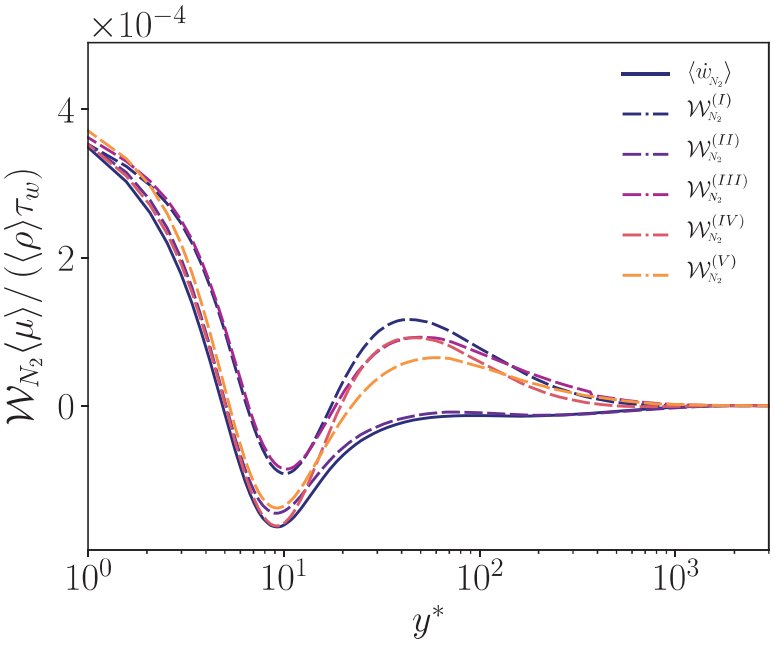

FIGURE 1. Wall-normal profiles of the chemical production rate for molecular nitrogen versus the semi-local wall-normal coordinate juxtaposed with the auxiliary variables $\mathcal{W}_{N_2}^{(\alpha)}$.

where the covariances among the mass fractions are retained in order to satisfy the continuity constraint $\sum_{i=1}^{N_s} Y_i = 1$. The wall-normal variation of the auxiliary chemical production rates expressed in Equations (2.2) through (2.5) are juxtaposed with the mean chemical production rates themselves in Figures 1-3, for which the integral over the sample space of the thermodynamic fluctuations is computed numerically via Monte Carlo integration instead of deterministic quadrature. That is, the integrals are directly evaluated by random sampling of the time-resolved DNS fields.

For all species in the reactive mixture, the laminar-closure approximation is shown to depart significantly from the corresponding mean chemical production itself. For molecular nitrogen in particular, the laminar closure results uniformly in an overprediction of the chemical formation rate while the impact of density fluctuations on the chemical production rate prove to be marginal, as evidenced by the minimal disagreement between $\mathcal{W}_{N_2}^{(II)}$ and $\langle\dot{w}_{N_2}\rangle$. On the basis of the close correspondence between $\mathcal{W}_{N_2}^{(I)}$ and $\mathcal{W}_{N_2}^{(III)}$ within the peak-temperature location, thermal fluctuations ostensibly represent the primary source of unresolved molecular nitrogen production within $y^* = 10$. Outside the peak-temperature location, however, fluctuations in both temperature and composition, as well as the correlations among the state variables, clearly have a significant impact on the chemical production rate, as $\mathcal{W}_{N_2}^{(III)}$, $\mathcal{W}_{N_2}^{(IV)}$, and $\mathcal{W}_{N_2}^{(V)}$ respectively exhibit clear departures from the mean chemical production rate outside the buffer layer.

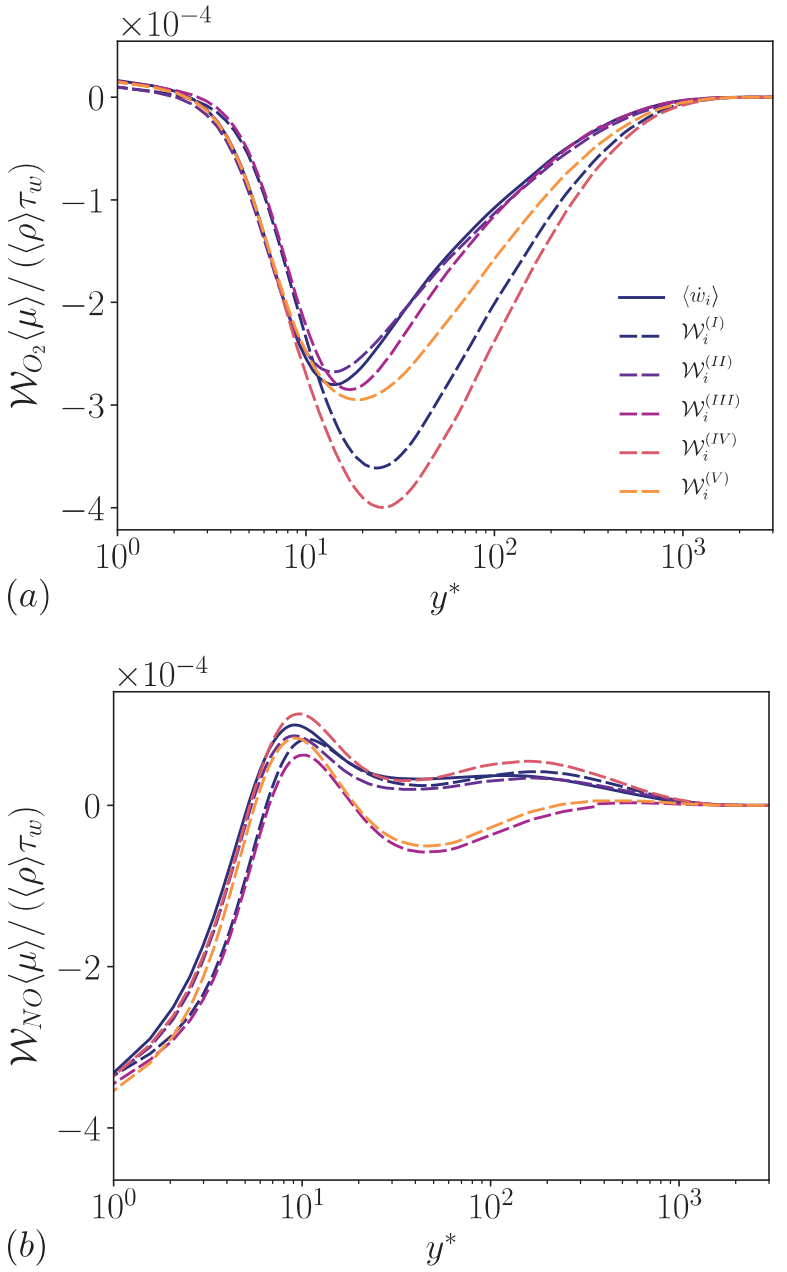

FIGURE 2. Wall-normal profiles of the chemical production rate versus the semi-local wall-normal coordinate juxtaposed with the auxiliary variables $\mathcal{W}_i^{(\alpha)}$ for (a) molecular oxygen, and (b) nitric oxide.

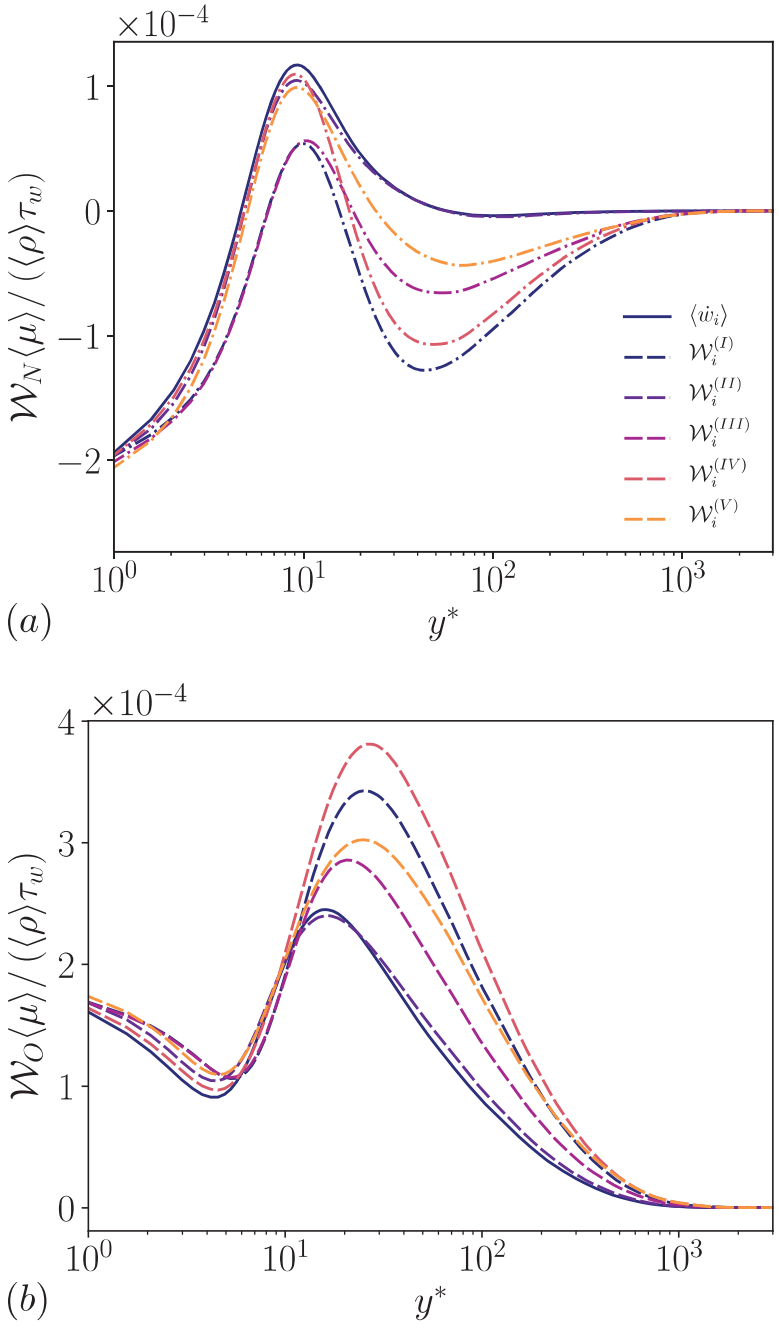

FIGURE 3. Wall-normal profiles of the chemical production rate versus the semi-local wall-normal coordinate juxtaposed with the auxiliary variables $\mathcal{W}_i^{(\alpha)}$ for (a) atomic nitrogen, and (b) atomic oxygen.

These characteristics observed in the molecular nitrogen production rate are also reflected in those of molecular oxygen, atomic nitrogen, and atomic oxygen. That is, while the effect of density fluctuations on the net chemical production rate is rather limited, thermal fluctuations are predominantly responsible for introducing unresolved chemistry within the peak-temperature location, while both thermal and compositional fluctuations prove consequential outside the buffer layer. In the particular case of atomic oxygen, $\mathcal{W}_O^{(IV)}$ proves to be an even worse approximation than the laminar closure itself owing to the nonzero correlation between temperature and molar-fraction fluctuations. For nitric oxide, however, temperature fluctuations remain the leading source of unresolved chemistry throughout the boundary layer, both inside and outside the peak-temperature location.

3. Scale-similar modeling of subgrid chemistry

Given the evident challenges associated with modeling turbulence-chemistry interactions in the RANS framework, the objective of present subsection is to assess the magnitude of, and present a modeling approach for, subgrid chemical production in the context of large-eddy simulation (LES). As such, let us define $\overline{(\cdot)}$ and $\widetilde{(\cdot)}$ as the filtering and Favre-filtering operators at the grid level of the filtered DNS, respectively. Moreover, let us propose an extension of the subgrid closure model of Jaberi & James (1998) by invoking the scale-similarity ansatz for each of the reactive sources as

$$\overline{\dot{w}_i} = \dot{w}_i\left(\overline{\rho}, \widetilde{T}, \{\widetilde{Y_j}\}\right) + C_i S_i, \qquad i = 1, 2, ..., N_s, \tag{3.1}$$

where C_i is an adaptive coefficient to be determined dynamically with the subgrid chemical residual modeled as proportional to

$$S_i = \overline{\dot{w}_i\left(\overline{\rho}, \widetilde{T}, \{\widetilde{Y_j}\}\right)} - \dot{w}_i\left(\overline{\overline{\rho}}, \widetilde{\widetilde{T}}, \{\widetilde{\widetilde{Y_j}}\}\right). \tag{3.2}$$

In this notation, $\overline{\overline{(\cdot)}}$ and $\widetilde{\widetilde{(\cdot)}}$ represent application of test-filtering and Favre-test-filtering operators to the grid-filtered fields, respectively. In order to recover continuity in this multi-component, multi-reaction system, let us further impose $C_1 = C_2 = ... \; C_{N_s} = C$ such that $\sum_{i=1}^{N_s} C_i S_i = 0$. Invoking Germano's identity (Germano *et al.* 1991) together with applying the method of least squares across the species' dimension, the dynamic coefficient appearing in the scale-similarity model can then be expressed solely in terms of grid-filtered and test-filtered fields as

$$C = \frac{\langle \sum_{i=1}^{N_s} S_i \mathcal{N}_i \rangle}{\langle \sum_{i=1}^{N_s} \mathcal{N}_i \mathcal{N}_i \rangle}, \tag{3.3}$$

where

$$\mathcal{N}_i = \overline{\dot{w}_i\left(\overline{\overline{\rho}}, \widetilde{\widetilde{T}}, \{\widetilde{\widetilde{Y_j}}\}\right)} - \dot{w}_i\left(\overline{\overline{\overline{\rho}}}, \widetilde{\widetilde{\widetilde{T}}}, \{\widetilde{\widetilde{\widetilde{Y_j}}}\}\right). \tag{3.4}$$

In this definition of $\mathcal{N}_i$, the symbols $\overline{\overline{\overline{(\cdot)}}}$ and $\widetilde{\widetilde{\widetilde{(\cdot)}}}$ denote application of a second test filter and Favre filter, respectively.

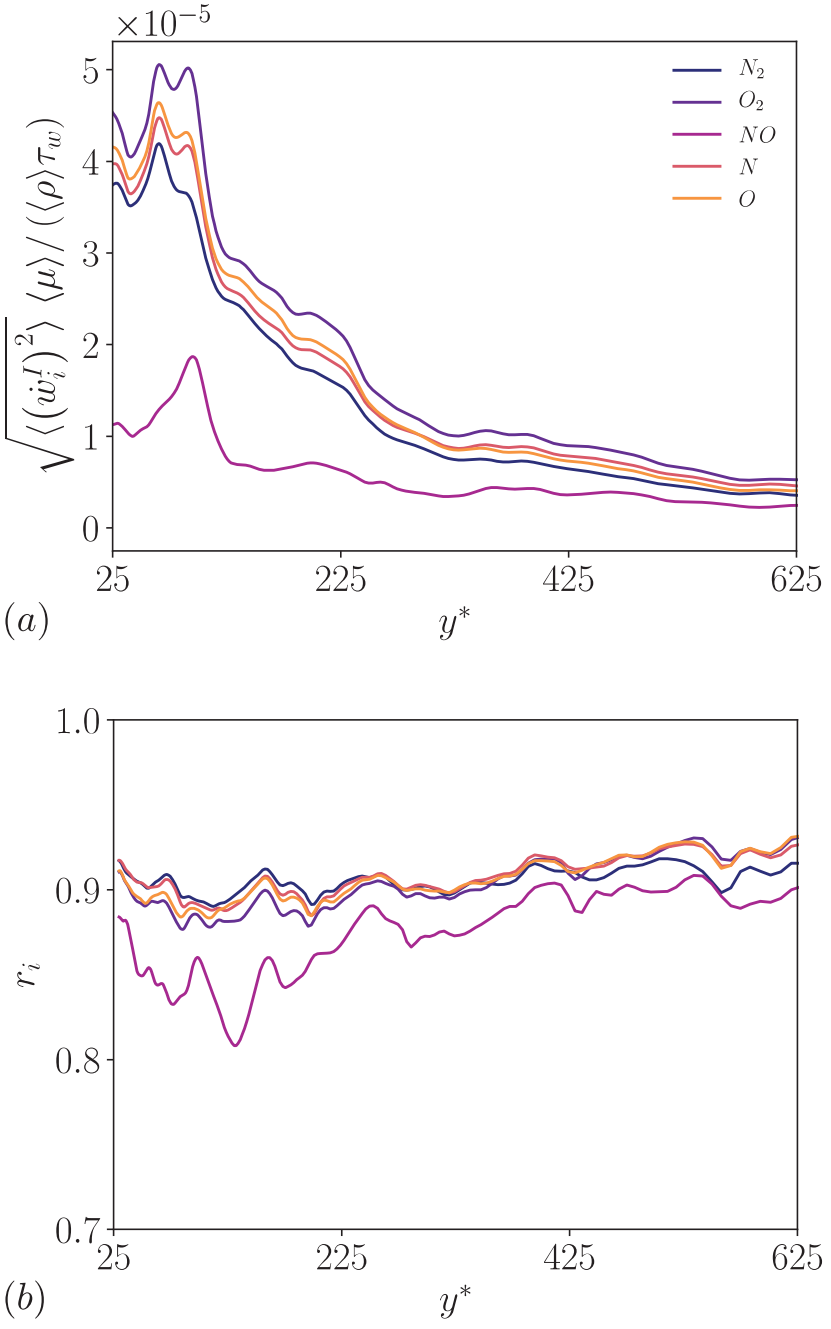

FIGURE 4. (a) Normalized r.m.s of subgrid chemical production rates and (b) correlation coefficient between scale similarity-model and exact closure from the filtered DNS with an effective filter width of 8Δ.

Figure 4 depicts the wall-normal variation in the normalized root mean square (r.m.s.) of the subgrid chemical production itself, $w_i^I = \overline{\dot{w}_i(\rho, T, \{Y_j\})} - \dot{w}_i(\overline{\rho}, \widetilde{T}, \{\widetilde{Y_j}\})$, together with the *a-priori* performance of the scale-similarity model as quantified by the correlation coefficients

$$r_i = \frac{\langle \dot{w}_i(CS_i)\rangle - \langle \dot{w}_i\rangle\langle CS_i\rangle}{\sqrt{(\langle \dot{w}_i^2\rangle - \langle \dot{w}_i\rangle^2)(\langle (CS_i)^2\rangle - \langle CS_i\rangle^2)}}. \tag{3.5}$$

The filtered DNS effective grid width is taken to be 8Δ where $\Delta = \sqrt[3]{\Delta x \Delta y \Delta z}$ is the nominal DNS grid size. The test filters utilized in the dynamic procedure likewise have widths 12Δ and 16Δ, respectively, and all of the filtering operations are performed with a top-hat kernel. Although the magnitude of the closure problem is clearly reduced relative to that of RANS, on account of the partial resolution of the reacting turbulence's length scales, significant portions of the chemical production rates remain subgrid. As observed in Figures 1-3, though, the impact of unresolved thermodynamic fluctuations is far more significant for the chemical production rate of both molecular and atomic oxygen and nitrogen than for nitric oxide. In particular for atomic oxygen, the r.m.s. of the subgrid chemical production rate is comparable to the overall filtered production rate itself for virtually all wall-normal locations within the boundary layer. Nevertheless, the scale-similarity model presented above proves very effective in estimating this subgrid reactive source term, achieving between 80% and 90% correlation with the exact residual of the chemical production rates. Clearly, modeling of this subgrid chemistry lends itself to application of the extended chemical scale-similarity model due to the lack of a characteristic chemical length scale, e.g., a flame thickness, in the reacting boundary layer. On account of its strong *a-priori* performance, then, the scale-similarity subgrid model represents a promising approach for addressing the hypersonic turbulence-chemistry interaction closure problem, though further *a-posteriori* analysis remains necessary.

4. Conclusions

Utilizing the DNS of Williams *et al.* (2023), the present study systematically characterizes turbulence-chemistry interactions in a strongly reacting hypersonic boundary layer. The Reynolds-averaged chemical production rates are shown to depart significantly from the corresponding laminar-closure approximations owing to turbulence-induced thermodynamic fluctuations and the strong non-linearity of the reactive source terms themselves. Interrogation of the DNS database likewise revealed that the unresolved chemistry cannot be attributed predominantly to thermal fluctuations but rather to joint fluctuations in all of the thermochemical state variables. The analagous closure problem in LES has been assessed *a priori* as well, with the r.m.s. subgrid chemical production rates representing a significant portion of the overall filtered production rates even for a moderate filter width. Utilizing a dynamic procedure to locally adapt its coefficient, the extended scale-similarity model proposed in the present work achieves very high correlations *a priori* with the filtered DNS results. Further assessment of this subgrid closure for the reactive source term via *a-posteriori* simulations will be addressed in future work.

Acknowledgments

Support from the National Science Foundation Graduate Research Fellowship Program under grant DGE-2146755 is acknowledged. This investigation was funded by the Advanced Simulation and Computing (ASC) program of the US Department of Energy's

National Nuclear Security Administration (NNSA) via the PSAAP-III Center at Stanford, Grant No. DE-NA0003968. C.T.W. thanks Ahmed Elnahhas and Dr. Mario Di Renzo for helpful discussions regarding this work.

REFERENCES

Bertin, J. & Cummings, R. 2006 Critical hypersonic aerothermodynamic phenomena. *Annu. Rev. Fluid Mech.* **38**, 129–157.

Candler, G. V. 2019 Rate effects in hypersonic flows. *Annu. Rev. Fluid Mech.* **5**, 379–402.

Di Renzo, M., Fu, L. & Urzay, J. 2020 HTR solver: An open-source exascale-oriented task-based multi-GPU high-order code for hypersonic aerothermodynamics. *Comput. Phys. Commun.* **255**, 107262.

Di Renzo, M. & Urzay, J. 2021 Direct numerical simulation of a hypersonic transitional boundary layer at suborbital enthalpies. *J. Fluid Mech.* **912**, A29.

Duan, L. & Martín, M.P. 2011a Effective approach for estimating turbulence-chemistry interaction in hypersonic turbulent boundary layers. *AIAA J.* **49**, 2239–2247.

Duan, L. & Martín, M.P. 2011b Assessment of turbulence-chemistry interaction in hypersonic turbulent boundary layers. *AIAA J.* **49**, 172–184.

Germano, M., Piomelli, U., Moin, P. & Cabot, W. 1991 A dynamic subgrid-scale eddy viscosity model. *Phys. Fluids A* **3**, 1760–1765.

Jaberi, F.A. & James, S. 1998 A dynamic similarity model for large eddy simulation of turbulent combustion. *Phys. Fluids* **10**, 1775-1777.

Martín, M.P. & Candler, G.V. 1999 Subgrid-scale model for the temperature fluctuations in reacting hypersonic turbulent flows. *Phys. Fluids* **11**, 2765–2771.

Martín, M.P. & Candler, G.V. 2001 Temperature fluctuation scaling in reacting boundary layers. AIAA Paper 2001-2717.

Park, C. 1990 *Nonequilibrium Hypersonic Aerothermodynamics*. Wiley.

Urzay, J. 2018 Supersonic combustion in air-breathing propulsion systems for hypersonic flight . *Annu. Rev. Fluid Mech.* **50**, 593–627.

Urzay, J. & Di Renzo, M. 2020 Engineering aspects of hypersonic turbulent flows at suborbital enthalpies. *Annual Research Briefs,* Center for Turbulence Research, Stanford University, pp. 7–32.

Vincenti, W. G. & Kruger C. H. 1965 *Introduction to Physical Gas Dynamics*. Wiley.

Williams, C. T., Di Renzo, M. & Moin, P. 2022 Computational framework for direct numerical simulation of shock-turbulence interaction in thermochemical nonequilibrium. *Annual Research Briefs,* Center for Turbulence Research, Stanford University, pp. 203–216.

Williams, C. T., Di Renzo, M. & Moin, P. 2023 Direct simulation of turbulence-chemistry interaction in a strongly reacting turbulent hypersonic boundary layer. *Annual Research Briefs,* Center for Turbulence Research, Stanford University, in press